

MESSENGER Magnetometer EDR-to-CDR Processing

Version 2i

27 April 2016

Prepared by
Haje Korth and Brian Anderson
The Johns Hopkins University
Applied Physics Laboratory
Laurel, MD 21784
USA

Document Review

Haje Korth, MESSENGER MAG Instrument Scientist, has reviewed and approved this document.

Change Log

DATE	SECTIONS CHANGED	REASON FOR CHANGE	REVISION
6/14/11	Change Log	Added change log.	V2d
6/14/11	12	Added information on changes incorporated in processing code versions 1.4, 1.5, and 1.6.	V2d
6/15/11	Document Review	Added document review information	V2e
3/7/16	1, 2, 3, 6, 7, 8, 12, 13, 15	Added offset temperature and duty cycle corrections corresponding to calibration software version 3.7; updated calibration software history; added appendix. Other minor final edits.	V2f
3/15/16	4, 13	Update SPICE kernel information. Minor edits to Version History introductory paragraph.	V2g
4/27/16	13	Added note on validation of final data set.	V2h
4/27/16	Various	Table numbering edits.	V2i

Table of Contents

1	Purpose.....	4
2	Introduction.....	4
3	Coordinate Systems	4
3.1	Sensor and Spacecraft Coordinates	4
3.2	J2000 Coordinates	5
3.3	Mercury Solar Orbital (MSO) Coordinates.....	5
3.4	Mercury Body Fixed (MBF) Coordinates.....	5
3.5	Radial-Tangential-Normal (RTN) Coordinates	6
4	SPICE Kernels	6
5	Time Latency Correction	7
6	Heater Correction.....	8
7	Offset Variation Correction	9
8	Absolute Calibration and Relative Alignment.....	15
9	UTC Conversion	15
10	Spacecraft Position Determination	16
10.1	Cartesian Coordinates	16
10.2	Spherical Coordinates	16
11	Coordinate System Transformation	17
12	Data Quality	18
13	Validation.....	18
14	Version History.....	19
15	References.....	21
16	Appendix.....	21

1 Purpose

This document provides a description of the conversion of MESSENGER Magnetometer Science (SCI) Experimental Data Records (EDRs) to Calibrated Data Records (CDRs). The processing steps described in this document represent the state of knowledge at the date of this document and were applied to the final mission dataset delivered to the PDS.

2 Introduction

The SCI EDRs are the raw data records used to derive magnetic field data used for scientific analysis. They contain 3-axis field samples from the magnetometer at the commanded sample rate as well as the Mission Elapsed Time (MET) and a range flag indicating the dynamic range the magnetometer operated in at the time of the observation. There are two dynamic ranges, a fine range of $\pm 1,530$ nT (range flag 0) and a coarse range of $\pm 51,300$ nT (range flag 1). Before the science data can be used for scientific analysis, the count rates in the EDRs must be converted to physical units and the data must be transformed into meaningful physical reference systems. This conversion yields calibrated data, which are stored in CDR data files. The processing steps from the EDR to the CDR level are described in this document and include:

- (1) accounting of time latency between the registered and actual times of the observation and conversion from spacecraft mission elapsed time (MET) to UTC;
- (2) subtraction of the temperature-dependent and sensor-heater thermally-induced magnetometer DC offsets for the three axes;
- (3) conversion from engineering units to physical units;
- (4) coordinate transformation from sensor to spacecraft coordinates and to other physical interplanetary and planetary reference frames;
- (5) assignment of a data quality flag to the observations.

3 Coordinate Systems

The calibrated data were transformed into several coordinate systems necessary for scientific analysis: J2000 inertial, Mercury Solar Orbital (MSO), Mercury Body Fixed (MBF), and Radial-Tangential-Normal (RTN). These coordinate systems are defined as follows. Position data in each system is included in the CDR products for J2000, MSO, MBF, and RTN coordinates.

3.1 Sensor and Spacecraft Coordinates

Sensor and spacecraft coordinates are defined as shown in Figure 1. In the spacecraft coordinate system, the Y-axis is parallel to the magnetometer boom axis with +Y directed from the spacecraft toward the MAG sensor; the X axis is parallel to the solar array rotation axis; the Z axis is orthogonal to X and Y and +Z points outward from the spacecraft adapter ring, and the +X direction completes the right handed system. The sensor axes are oriented nearly parallel to the spacecraft axes. The transformation between the two coordinate systems is reported in the magnetometer instrument paper [Anderson *et al.*, 2007].

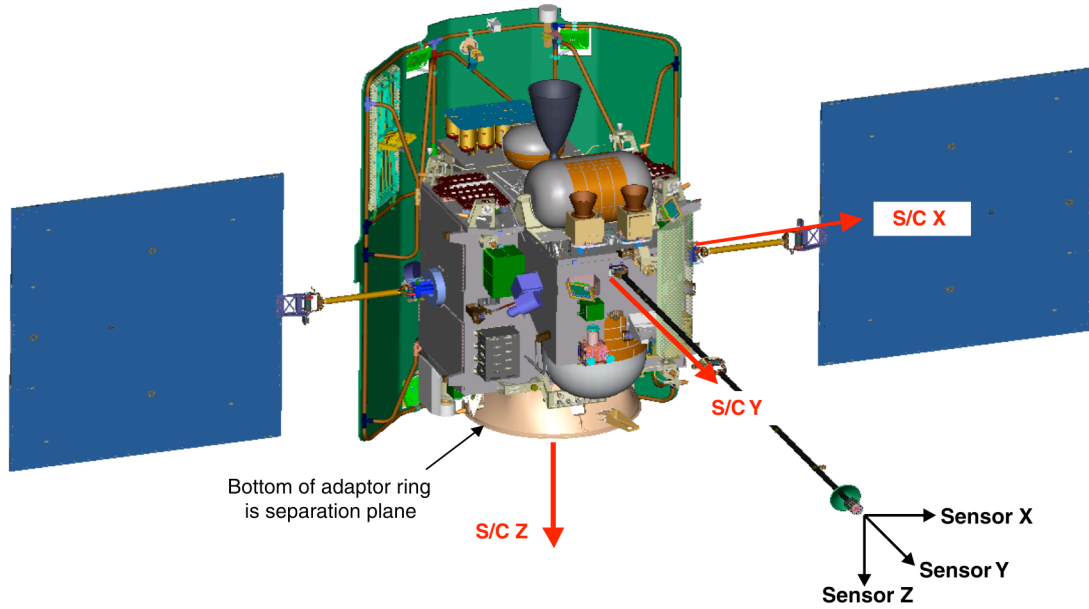


Figure 1: Definition of sensor and spacecraft coordinates.

3.2 J2000 Coordinates

In this coordinate system, the +X-axis points toward the mean vernal equinox, +Z points along the mean rotation axis of the Earth on 1 Jan 2000 at 12:00:00.00 Barycentric Dynamical Time (TDB), which corresponds to JD 2451545.0 TDB, and Y completes the right-handed system.

3.3 Mercury Solar Orbital (MSO) Coordinates

In this coordinate system, the +X-axis points from Mercury center toward the Sun, +Z points northward perpendicular to Mercury's orbit plane, and Y completes the right hand system nominally directed opposite Mercury's orbital velocity around the Sun. SPICE constructs the MSO coordinate system in the following manner: it computes the position of the Sun as viewed from Mercury and labels this as the +X-axis. Then it computes the projection of the velocity of Mercury as viewed from the Sun into the plane normal to the already defined X-axis and forces this to be the -Y-axis of the MSO frame. The Z-axis is defined by completing the right-handed axes triple (i.e. the cross product of X with Y). The Venus-centered Venus solar orbital (VSO) coordinate system is similarly defined.

3.4 Mercury Body Fixed (MBF) Coordinates

The MBF coordinate system is defined by the planetocentric position, Cartesian X, Y, Z coordinates related to the planetocentric distance, r , the latitude, λ , measured positive northward from the equator, and the longitude, φ , measured positive eastward from the prime meridian. The cartesian X, Y, Z coordinates are: $x_{MBF} = r \cdot \cos(\varphi) \cdot \cos(\lambda)$, $y_{MBF} = r \cdot \sin(\varphi) \cdot \cos(\lambda)$, $z_{MBF} = r \cdot \sin(\lambda)$. The unit e_{MBF} components, $e_{x_{MBF}}$, $e_{y_{MBF}}$ and $e_{z_{MBF}}$ are defined simply as: $e_{x_{MBF}} = X_{MBF}/r$, $e_{y_{MBF}} = Y_{MBF}/r$, $e_{z_{MBF}} = Z_{MBF}/r$.

3.5 Radial-Tangential-Normal (RTN) Coordinates

In RTN coordinates, R points from Sun center to the spacecraft. T is formed by the cross product of the solar rotation axis and R and lies in the solar equatorial plane. N is formed by the cross product of R and T and is the projection of the solar rotational axis on the plane of the sky.

4 SPICE Kernels

The MESSENGER project adopted the SPICE information system to assist science and engineering planning and analysis. SPICE is developed by the Navigation and Ancillary Information Facility (NAIF) under the directions of NASA's Science Directorate. The SPICE toolkit is available at the NAIF web site (<http://naif.jpl.nasa.gov>) in the compiled programming languages FORTRAN and C. Interfaces to higher-level data analysis software, e.g., Interactive Data Language (IDL) and Matlab, are also provided. The MESSENGER MAG CDR processing routines were written in IDL using the toolkit provided by NAIF.

The primary SPICE data sets are kernels. SPICE kernels are composed of navigation and other ancillary information structured and formatted for easy access. SPICE kernels were generated by the most knowledgeable technical contacts for each element of information. Definitions for kernels include or are accompanied by metadata, consistent with flight project data system standards, which provide pedigree and other descriptive information needed by prospective users.

The following SPICE kernel files were used to compute the UTC time and any geometric quantities found in the PDS labels. Kernel files were generated throughout the mission with a file-naming convention specified by the MESSENGER project. The SPICE kernels are archived separately in the SPICE data volume with the VOLUME_SET_NAME "MESSENGER: GEOMETRY" and the VOLUME_SET_ID "USA_NASA_PDS_MESSNAIF_1001".

*.bsp:

MESSENGER spacecraft ephemeris file. Also known as the Planetary Spacecraft Ephemeris Kernel (SPK) file.

*.bc:

MESSENGER spacecraft orientation file. Also known as the Attitude C-Kernel (CK) file.

*.tf:

MESSENGER reference frame file. Also known as the Frames Kernel. Contains the MESSENGER spacecraft, science instrument, and communication antennae frame definitions.

*.ti:

MESSENGER instrument kernel (I-kernel). Contains references to mounting alignment, operating modes, and timing as well as internal and field of view geometry for the MESSENGER Magnetometer.

*.tsc:

MESSENGER spacecraft clock coefficients file. Also known as the Spacecraft Clock Kernel (SCLK) file.

*.tpc:

Planetary constants file. Also known as the Planetary Constants Kernel (PcK) file.

*.tls:

NAIF leapseconds kernel file. Used in conjunction with the SCLK kernel to convert between Universal Time Coordinated (UTC) and MESSENGER Mission Elapsed Time (MET). Also called the Leap Seconds Kernel (LSK) file.

This kernel set used in generating a CDR is listed in the release notes for the produced CDR.

5 Time Latency Correction

As described in *Anderson et al.* [2007], the time stamps in the EDR records are delayed with respect to the actual time of the magnetic field observations due to onboard filtering of the data and intrinsic delay in the instrument feedback response. The net time lag depends on the sample rate and is given in Table 1 from *Anderson et al.* [2007]. These values listed in the “net lag” column are subtracted from the MET associated with the vector sample in the EDR.

Rate setting	Sample rate (s ⁻¹)	Filter: -3 dB (Hz)	Attenuation (dB/octave)	IIR lag (s)	Net lag (s)
0	0.01	0.567*	-72*	2.316	2.358
1	0.02	"	"	"	"
2	0.05	"	"	"	"
3	0.10	"	"	"	"
4	0.20	"	"	"	"
5	0.50	"	"	"	"
6	1.00	"	"	"	"
7	2.0	1.141*	-73*	1.144	1.186
8	5.0	2.83*	-97*	0.435	0.477
9	10.0	5.38*	-147*	0.181	0.223
10	20.0	11.3	-17	0.0	0.042

*Characteristics of IIR digital filter

Table 1: MESSENGER Magnetometer sample rates, digital IIR filter -3 dB points, filter attenuation characteristics, IIR time lags, and net time lags.

6 Heater Correction

Data judged to be valid data (see MAG CDR confidence level note in MAGCDR_DS.CAT) are subject to contributions from temperature dependent zero-levels and signals related to sensor survival-heater operation. This section describes the time-dependent signals due to heater operation and specifically those commensurate with the heater cycle period. A contamination signal associated with the magnetometer heater operation with the same period as the heater-cycle period and synchronized with heater operation is superimposed on magnetometer data when the heater was operating. The origin of the periodic contamination signal is not entirely known but is presumed to be due to variations in temperature gradients within the sensor. The contamination is manifested as perturbations with the periodicity of the 100-s heater control period. The magnitude and waveform of the offset variations is different for each of the three axes and depends on the heater duty cycle. Effects of the thermal environment and heater duty-cycle changes on the zero-levels or offsets are covered in Section 7.

During cruise after 9 March 2007 when operations were started with version 10 of the MAG EPU software (see MAG CDR confidence level note), the sensor was in darkness and the heater typically operated at a duty cycle of 40%, i.e., at full power for 40 seconds and then off for 60 seconds. The heater state (on/off bit) is captured in the MAG log AC data stream (LAC) EDRs at a time resolution of one second, corresponding to the one-second command iteration at which this state was changed via command to the spacecraft. The heater state bit was used to construct the average time behavior versus time within the 100 second heater period using a superposed epoch analysis of all data acquired in the solar wind binned by heater duty cycle in 4% wide bins

for bin centers from 12% to 40%. The bins start at 10% because the spacecraft required a 10-count persistence in a change of the heater state bit before turning the heater either on or off. Thus, any duty cycle below 10% was ignored by the spacecraft. In addition, this leads to a 10-s delay between the heater request bit and the actual heater power state change.

The results of the superposed epoch analysis are shown in Figure 2 for the sensor X, Y, and Z axes. The 10-s delay is obvious as is the flat profile for duty cycles below 10%. In addition, there is a regular evolution in the shape and amplitude with increasing duty cycle. The largest signal is in the Y-axis and is just under 0.75 nT in peak-to-peak amplitude. The discrepancies between the spline fits and the averages are less than 0.1 nT or 2 DN. The spline fits in units of counts or DN versus heater cycle time are given in the Appendix.

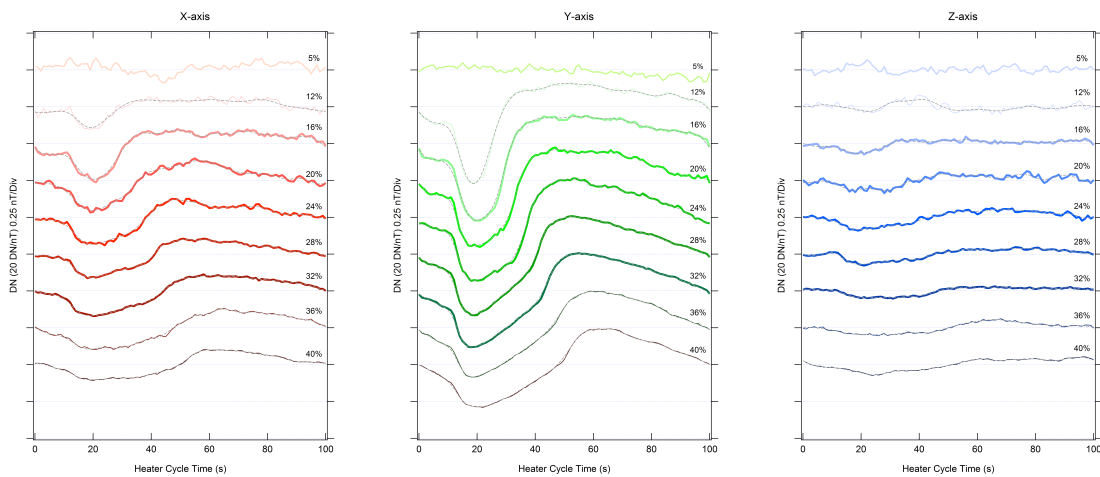


Figure 2. Superposed epoch averages of solar wind observations from all orbital mission phase data versus time during the 100-s period heater operation for a range of duty cycles from 0% (top) to 40% (bottom). Colored traces show the averages and dashed curves are the spline fits which were used to construct a continuous representation for the perturbations within each duty cycle. From left to right panels show response for the sensor X, Y, and Z axes, respectively.

To obtain a continuous function for the heater-cycle time profile, the start time of the heater period was identified from the rising edge in the heater bit time series. If the persistence was at least 10 s, then a waveform was interpolated both in time and duty cycle from the curves in Figure 2 to the actual time and duty cycle. Linear interpolation was used between duty-cycle bins and the derivative of the duty-cycle signal at a given heater-cycle time derived from the 12% and 16% bins was used to extrapolate below 12%. Similarly, the derivative obtained between the 36% and 40% bins was used to extrapolate above 40%.

7 Offset Variation Correction

The thermal environment of the magnetometer sensor was substantially different during orbital operations than it was during cruise. During cruise after final implementation of the software heater controller, the sensor temperature was regulated to remain near -50°C . The cruise offset

calibration is valid for this temperature and the mean heater duty cycle required when the sensor was in the spacecraft shadow. As a result, the net offset during cruise was constant. In Mercury orbit however, the sensor was exposed to radiant heat from the planet, which was most intense at low altitudes on the dayside, as well as conducted and radiant heat from the magnetometer sun shade when the spacecraft was tilted to accommodate remote-sensing observations. As a result, the heater duty cycle varied from its nominal cruise value and maximum of near 40% to 0% whenever the sensor temperature warmed above -50°C , which occurred on most orbits. During the final year of the mission, the sensor temperature occasionally exceeded $+30^{\circ}\text{C}$ at the lowest altitudes.

The temperature and duty-cycle variations principally impact the zero levels or offsets of the magnetometer. Denoting the readings (counts) in the X, Y, and Z axes by c_x , c_y , and c_z and the variable offsets as $c_{x0}(T,d)$, $c_{y0}(T,d)$, and $c_{z0}(T,d)$, where T is the temperature and d is the heater duty cycle, the corrected data counts $c_{x,C}$, $c_{y,C}$, and $c_{z,C}$ in sensor coordinates are given by

$$\begin{aligned} c_{x,C} &= c_x - c_{x0}(T, d) \\ c_{y,C} &= c_y - c_{y0}(T, d) \\ c_{z,C} &= c_z - c_{z0}(T, d) \end{aligned} \quad (1)$$

The duty cycle only varies when the sensor temperature is regulated at -50°C , and the temperature only varies when the heater is not being used so that the functional form for the offsets may be written as

$$c_{j0}(T, d, t) = c_{j0,d}(d, t) + (c_{j0,T}(T(t)) - c_{j0,T}(-50^{\circ}\text{C})) \quad (2)$$

where j denotes the sensor axis X, Y, or Z, and the subscripts ‘d’ and ‘T’ denote offsets related to the heater duty cycle and sensor temperature, respectively. Because the average solar-wind magnetic field vector is zero, we used long-term averages of data acquired in the solar wind binned either temperature or duty cycle to determine $c_{j0,T}$ and $c_{j0,d}$, respectively.

For $c_{j0,T}$, data acquired when the duty cycle was 0% and the spacecraft was resident in the solar wind were binned by temperature in 10°C -wide bins, and all data in a given temperature bin were averaged. These averages yield estimates of the offset as a function of temperature. These averages and fits to the results are shown in Figure 3. The offsets vary slowly with temperature below -10°C and more rapidly above -10°C so two-segment linear fits were used to represent continuous variation of offset with temperature. The fits used the square root of the number of samples in each bin as a weight for each point and there were very few samples in the upper two temperature bins, which accounts for the apparent departure of these averages from the fits.

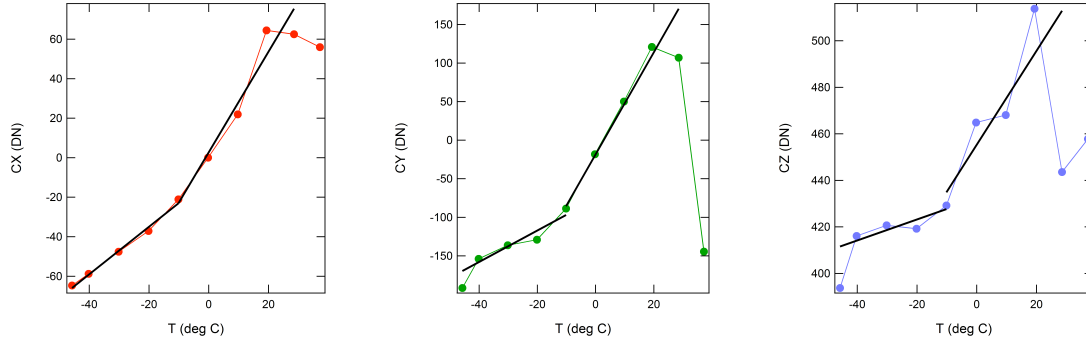


Figure 3. Long-term averages of solar wind observations versus sensor temperature from all orbital-mission-phase data with the sensor heater off. From left to right panels show response for the sensor X, Y, and Z axes, respectively.

The fits were implemented using two linear functions joined at a middle temperature, T_m , written as

$$c_{j,0T} = A_{0j} + B_{0j}T \quad \text{for } T \leq T_{mj} \quad (3a)$$

$$c_{j,0T} = A_{1j} + B_{1j}T \quad \text{for } T \geq T_{mj} \quad (3b)$$

where $j = x, y, \text{ or } z$, T is in $^{\circ}\text{C}$, and T_m is the temperature where the two linear functions match given by

$$T_{mj} = (A_{0j} - A_{1j}) / (B_{1j} - B_{0j}) \quad (4)$$

The coefficients for all three axes for equations (3a) and (3b) are given in Table 2.

Table 2. Coefficients for offsets as functions of sensor temperature.

Axis	A_0	B_0	A_1	B_1	$T_m (^{\circ}\text{C})$
x	-10.802	1.2043	2.8435	2.5445	-10.1817
y	-76.138	2.042	-18.176	6.6181	-12.6662
z	432.27	0.45175	455.4	2.016	-14.7866

To determine the $c_{j,0,d}$, all data in each 100-s heater operation period with a finite duty cycle and when the spacecraft was resident in the solar wind were binned by duty cycle in 4% wide bins. Data within a given duty cycle bin were averaged to obtain estimates for the offset variation with duty cycle. The results of these averages are shown in Figure 4 together with linear fits to these data constrained to yield the values for $c_{j,0,T}(-50^{\circ}\text{C})$. For duty cycles below 20% and above 35%, there were relatively few points, which together with the $d = 0$ value constraint accounts for the departures of the data from the linear fits. The fits used the square root of the number of samples in each bin as a weight for each point. In addition, the intercept at 0 duty cycle was held fixed to the -50°C values for the offsets versus temperature. The values at $d = 0$ in Figure 3 are actually obtained for all values of d from 1 through 99 which correspond to no heater use and are

plotted at $d = 0$. As one expects, the averages for $d = 0$ closely correspond to the results for the temperature offset dependencies at -50°C .

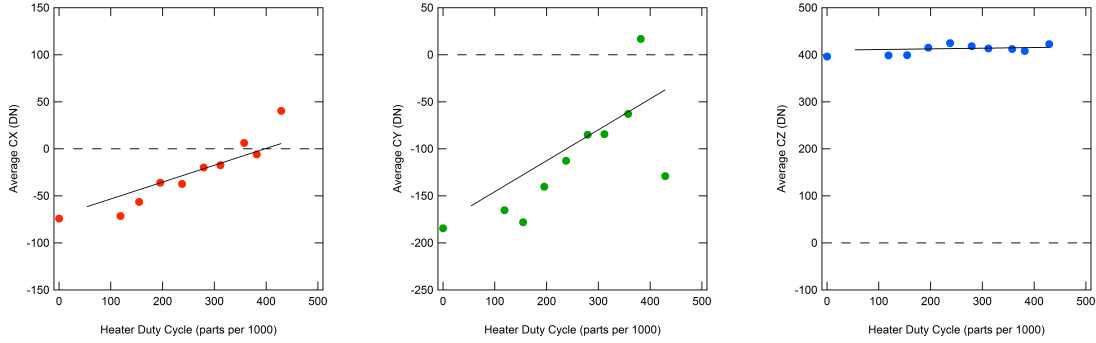


Figure 4. Long term averages of solar wind observations versus sensor heater duty cycle (in parts per 1000) from all orbital mission phase data with finite heater duty cycles. From left to right panels show response for X, Y, and Z axes, respectively.

The linear fits to the offset with duty cycle represent the level shifts in the offsets but do not capture the time dependence of the change from one duty cycle to another. The variation of offsets with duty-cycle offset were represented with simple line fits

$$c^*_{j,0d} = C_{0j} + D_{0j}d \quad \text{for } d \geq 100 \quad (5a)$$

$$c^*_{j,0d} = 0 \quad \text{for } d < 100 \quad (5b)$$

where d is in parts per 1000 and the coefficients are given in Table 3. The asterisk indicates that equation (5) gives the level shift in the offsets that occurs in steady state and does not capture the time dependence when the duty cycle changes.

Table 3. Coefficients for offsets as functions of heater duty cycle.

Axis	* C_0	† D_0
x	-71.0	0.17885
y	-178.2	0.32851
z	409.7	0.01477

* Units for C_0 are counts and the relationship to nT is covered in Section 9.

† Units for D_0 are counts per unit duty cycle, where d is in parts per 1000.

The thermal controller in version 10 of the MAG EPU software evaluated the heater duty cycle once every ten heater periods, i.e. every 1000 s, and a change in duty cycle was requested at this interval, which corresponds to a shift in the steady state offsets. During orbital operations, the duty-cycle changes were often substantial so that the changes in $c^*_{j,0d}$ could be as large as 30 counts or more, corresponding to ~ 1.5 nT. Physically, the thermal gradients adjust continuously from their value at one duty cycle to a new value with a characteristic relaxation time. Ignoring this behavior and applying corrections with discontinuities would introduce spurious steps in the

data. Thus, it was essential to characterize the time dependence of the transitions in applied duty cycle.

The relaxation time was characterized by accumulating statistics on changes in the duty cycle in a superposed epoch analysis but using a 1200 second interval that was chosen to start 200 seconds prior to a change in the duty cycle. Because the trend of offset with duty cycle is linear, all steps of the duty cycle could be accumulated together and normalized for the duty cycle change. In addition, positive and negative changes in d were combined accounting for opposite signs of the step in the data. Because the dependence of offset on duty cycle is strongest for the Y-axis, the results of this analysis were the most definitive for the Y-axis and yield a time constant, τ , of 872 seconds.

This result implies that in a 1000-s interval of fixed duty cycle, the offsets reach roughly 70% of the difference between the old and new offsets. One cannot assume that the new steady state value has been attained when a new duty cycle value is commanded but must calculate the offset value achieved at 1000 seconds from the last change and use this as the new starting point for the next relaxation time. Note that at any given change in duty cycle the steady state offset does not correspond to the actual offset value. However, if one assumes that the sensor acquired its steady state offsets at some time in the distant past, say at least 5000 seconds prior, and then track the actual time dependence over that time to the present, the error in the initial assumption becomes negligible. For a time constant of 872 seconds the error is less than 0.3% of the initially assumed offset value, or less than 1 DN. Using this approach, the time-dependent offset was evaluated as follows. Using a 5000 second ‘look back’ interval, we let:

- $o_{c,d}(t)$ = the time dependent offset value in DN;
- t_s = the time of the current sample in seconds;
- dt = time delay between the heater bit lo to hi transition and the actual onset of heater board power (10 seconds);
- t_0 = the time of the most recent change in the duty cycle in seconds;
- c^*_0 = the steady state offset value from equation (5) in DN corresponding to the duty cycle that was set at t_0 ;
- t_1 = the time of the first duty cycle change prior to t_0 ;
- c^*_1 = the steady state offset value from equation (5) in DN corresponding to the duty cycle that was set at t_1 ;
- t_2 = the time of the first duty cycle change prior to t_1 ;
- c^*_2 = the steady state offset value from equation (5) in DN corresponding to the duty cycle that was set at t_2 ;
- t_3 = the time of the first duty cycle change prior to t_2 ;
- c^*_3 = the steady state offset value from equation (5) in DN corresponding to the duty cycle that was set at t_3 ;

- t_4 = the time of the first duty cycle change prior to t_3 ;
 c_4^* = the steady state offset value from equation (5) in DN corresponding to the duty cycle that was set at t_4 ;
 t_5 = the time of the first duty cycle change prior to t_4 ;
 c_5^* = the steady state offset value from equation (5) in DN corresponding to the duty cycle that was set at t_5 ;

The offset at t_s is then calculated by the following sequence of operations performed in order 6a through 6f which yield estimates for the actual offsets at times t_4 , t_3 , t_2 , t_1 , t_0 and finally t_s , denoted c_{t4} , c_{t3} , c_{t2} , c_{t1} , c_{t0} , and $c(t_s)$, respectively. Note that these are not equations in the mathematical sense but assignment statements denoted by the ' \leftarrow ' symbol.

$$c_{t4} \leftarrow c_5^* \{ 1 - \exp(-\max(t_4 - t_5 - dt, 0)/\tau) \} \quad (6a)$$

$$c_{t3} \leftarrow c_4^* - (c_4^* - c_{t4}) \exp(-(t_3 - t_4 - dt, 0)/\tau) \quad (6b)$$

$$c_{t2} \leftarrow c_3^* - (c_3^* - c_{t3}) \exp(-(t_2 - t_3 - dt, 0)/\tau) \quad (6c)$$

$$c_{t1} \leftarrow c_2^* - (c_2^* - c_{t2}) \exp(-(t_1 - t_2 - dt, 0)/\tau) \quad (6d)$$

$$c_{t0} \leftarrow c_1^* - (c_1^* - c_{t1}) \exp(-(t_0 - t_1 - dt, 0)/\tau) \quad (6e)$$

$$c(t_s) \leftarrow c_0^* - (c_0^* - c_{t0}) \exp(-(t_s - t_0 - dt, 0)/\tau). \quad (6f)$$

We then set

$$c_{j0,d}(d, t) = c(t_s) \quad (7)$$

which is used in Equation 2 to obtain the total offset correction as a function of time. This calculation effectively assumes that the offset prior to t_5 was zero which results in an error no larger than $200 \exp(-5000/\tau) = 0.6$ DN which we neglect.

Equation (2) yields valid offsets for all data after implementation of the 100-s heater period with MAG EPU software version 10, which occurred on 9 March 2007 and which spans a period four years prior to orbit insertion including all three Mercury gravity-assist encounters by MESSENGER.

There are no mission requirements for MAG data accuracy prior to observations at Mercury. Prior to 9 March 2007, data acquired with the MAG sensor in shadow behind the spacecraft either have uncorrectable noise due to contamination from interference effects of the heater operating in hardware regulation or operating at -50°C in software regulation but with a 1000-s period. In addition, data acquired prior to boom deployment on 8 March 2005 contain uncorrectable noise from the spacecraft. Data acquired after boom deployment with the MAG sensor in sunlight are free of both heater-related contamination and spacecraft magnetic noise and are useful for science analyses of the interplanetary magnetic field. Under these conditions,

the mean sensor temperature was 22.4°C with minimal variation (less than 10°C) with a standard deviation of 4.2°C. The offsets from equation (2) with this temperature were used for these data.

8 Absolute Calibration and Relative Alignment

The conversion from counts, corrected for offsets, to physical units of nano-Tesla is described by *Anderson et al.* [2007]. Using the sensor readings corrected for the temperature and duty cycle dependent offsets, the magnetic field in sensor coordinates can be written as

$$\begin{aligned} B_x &= k_x c_{x,C} \\ B_y &= \alpha k_x c_{x,C} + k_y c_{y,C} \\ B_z &= \beta k_x c_{x,C} + \gamma k_y c_{y,C} + k_z c_{z,C} \end{aligned} \quad (8)$$

where k_x , k_y , and k_z are the gain coefficients for each axis and α , β , and γ measure the contributions of X in the Y axis, X in the Z axis, and Y in the Z axis, respectively. The parameters from the ground calibration are shown in Table 4 [*Anderson et al.*, 2007] and are insensitive to temperature.

Parameter	Coarse range (±51,300 nT)	Fine range (±1,530 nT)
k_x : nT/count	1.56513	0.046769
k_y : nT/count	1.56419	0.046673
k_z : nT/count	1.61029	0.047997
α	-0.00462	-0.00462
β	0.00053	0.00053
γ	-0.00736	-0.00736
X offset: counts (nT)	-30.4 (-48)	-1017 (-48)
Y offset: counts (nT)	-75.2 (-118)	-2520 (-118)
Z offset: counts (nT)	-16.2 (-26)	-544 (-26)

Table 4: Absolute gain, sensor alignment, and internal pre-launch offsets.

9 UTC Conversion

The UTC conversion from MET to UTC is handled by the SPICE toolkit using the following IDL commands:

```
cspice_scs2e, sc_id, met_str, et
```

```
cspice_timeout, et, 'YYYY DOY HR MN SC.###', 21, time_str
```

The routine `cspice_scs2e` converts the MET into ephemeris time `et` native to SPICE, whereby the spacecraft ID for MESSENGER is -236. The routine `cspice_timeout` then convert the ephemeris time `et` to a UTC time string which is associated with the observation.

10 Spacecraft Position Determination

10.1 Cartesian Coordinates

The spacecraft position for each MET is returned by the SPICE toolkit using the following IDL commands:

```
cspice_scs2e, sc_id, met_str, et
cspice_spkpos, target, et, frame, correction, observer, position, ltime
```

The routine `cspice_scs2e` converts the MET into ephemeris time native to SPICE using the MESSENGER spacecraft ID which is -236. The routine `cspice_spkpos` then acquires the position of the spacecraft for the ephemeris time `et` given the target, frame, light-time correction, and observer. Since we are interested in the UTC at the spacecraft, the position of MESSENGER with respect to the Sun in J2000 coordinates is obtained without light-time correction using:

```
cspice_spkpos, 'MESSENGER', et, 'J2000', 'NONE', 'SUN', position, ltime
```

The position of MESSENGER in the Mercury-centric MSO coordinate system without light-time correction can be obtained using:

```
cspice_spkpos, 'MESSENGER', et, 'MSGR_MSO', 'NONE', 'MERCURY',
position, ltime
```

The position of MESSENGER in Mercury body-fixed coordinates without light-time correction can be obtained using:

```
cspice_spkpos, 'MESSENGER', et, 'IAU_MERCURY', 'NONE', 'MERCURY',
position, ltime
```

10.2 Spherical Coordinates

When transforming the magnetic field samples to Radial-Tangential-Normal (RTN) coordinates, the spacecraft coordinates are more appropriately represented in the following spherical coordinates: (1) radial distance of the MESSENGER spacecraft from the Sun in units of km; (2) northward latitude of the MESSENGER spacecraft above instantaneous ecliptic plane in units of

degrees; (3) Azimuth angle of the MESSENGER spacecraft in the instantaneous ecliptic plane with respect to the Earth-Sun line in units of degrees, positive in direction of the Earth's orbital motion. The components are computed as follows:

Radial component:

```
cspice_spkpos, 'MESSENGER', et, pframe, 'NONE', observer, m_pos, ltime
pos_r=cspice_vnorm(m_pos)
```

Northward Latitude:

```
cspice_spkezr, 'EARTH', et, pframe, 'NONE', observer, state, ltime
cspice_vcrss, state[0:2], state[3:5], es_norm
pos_lat=90-cspice_vsep(es_norm, m_pos)/!dtor
```

Azimuth:

```
cspice_vperp, state[3:5], state[0:2], ve_espl_proj
cspice_psv2pl, state[0:2], state[0:2], state[3:5], es_plane
cspice_vprjp, m_pos, es_plane, m_espl_proj
sign=sgn(cspice_vdot(ve_espl_proj, m_espl_proj))
pos_az=sign*cspice_vsep(state[0:2], m_espl_proj)/!dtor
```

11 Coordinate System Transformation

The coordinate transformation from MESSENGER MAG sensor coordinates to J2000, MSO, and MBF coordinates is handled by the SPICE toolkit using the following IDL commands:

```
cspice_scs2e, sc_id, met_str, et
cspice_pxform, frame1, frame2, et, xform
cspice_mxv, xform, b_sensor, b_rot
```

The routine `cspice_scs2e` converts the MET into ephemeris time native to SPICE, using the spacecraft ID for MESSENGER, -236. The routine `cspice_pxform` gives the transformation matrix between the coordinate system of origin, `frame1`, and the target coordinate system, `frame2`, at a given ephemeris time, `et`. The coordinate system of origin for MAG after boom deployment is `MSGR_MAG`. The coordinate system of MAG prior to boom deployment is accessed using `MSGR_MAG_STOWED`. The target coordinate systems for the CDRs are J2000, `MSGR_MSO`, `IAU_MERCURY`, and `MSGR_RTN` for transformations into J2000, MSO, MBF, and RTN coordinates, respectively. Finally, the `cspice_pxform` routine performs the actual coordinate system transformation by multiplying the transformation matrix with the observations in the coordinate system of origin. For example, the transformation from the MAG sensor coordinate system into MSO coordinates is executed using:

```
cspice_pxform, 'MSGR_MAG', 'MSGR_MSO', et, xform
cspice_mxv, xform, b_sensor, b_mso
```

12 Data Quality

The final step in the conversion of experimental to calibrated data records is the assignment of the data quality flag to the observations. The MAG data quality flag is a three digit code, denoted as SHC, which is defined in Table 5. S indicates the configuration of the sensor. H indicates the sensor survival heater control mode being used. C indicates the presence of contamination in the data and whether contamination, if present, is judged to be correctable to meet the science requirement of 1 nT. For example, a data quality flag of ‘100’ indicates: that the boom was deployed with the sensor facing the sun, that the heater operated in hardware regulation, and that no contamination signals are known to be present. The data quality flag will be assigned via a lookup table, which is maintained during validation of the data set.

Table 5: MAG data quality flag definitions.

S: Sensor Configuration	Definition
0	Sensor stowed – prior to boom deployment
1	Boom deployed – SC +Y axis to Sun - sensor in sunlight
2	Boom deployed – SC –Y axis to Sun - sensor in shadow

H: Heater Mode	Definition
0	Hardware regulation (MAG FSW V8)
1	Software regulation version 1 (MAG FSW V9)
2	Software regulation version 2 (MAG FSW V10)

C: Contamination	Definition
0	No contamination signals known to be present
1	Uncorrectable contamination signals present
2	Contamination signals present but corrected in EDR to CDR conversion.

13 Validation

As a consequence of the thermal baseline correction, the sensor offsets in the final CDR data set are time variable. To ensure that the complex baseline correction was applied correctly, the time series of the sensor offsets were examined for smoothness. The thermal baseline was computed from data recorded at different intervals in distinct EDR files, and the correction required proper alignment of the various time series as well as consideration of details in the instrument flight software implementation. Incorrect implementation of the baseline correction was typically manifested in discontinuities in the offset time series. Evaluation of the smoothness of the

baseline correction proved effective for detecting shortcomings of the algorithms applying the correction as defined in sections 6 and 7. Final automated product validation confirmed smooth offset variations and thus correct implementations of the calibration algorithm.

The calibrated magnetic field components in the final CDR data set differ from those in the CDR V6 data set delivered previously to the PDS by up to 10%. Because the difference in the values from the previous data set are not negligible, important scientific results derived from Magnetometer data and published over the course of the mission have been reassessed to determine to impact on the scientific conclusions. This analysis included the quantities describing the nature of Mercury's low-order planetary field. It was found that the thermal baseline correction yields changes that are well within the uncertainties quoted in the published studies.

14 Version History

The conversion from the EDR to the CDR level was evolutionary. CDR files were reprocessed when (1) the MAG calibration changed, (2) the MAG team found it necessary or desirable to change the file format, or (3) when bugs in the processing software were identified. The reprocessed CDR files and the MAG EDR2CDR processing software were both given new version number reflecting the changes. Version numbers for CDRs and processing software may differ from each other. For this reason the version number of the processing software was captured in the CDR label. Below is the summary of the version history of the MAG EDR2CDR processing software.

v1.0 (04/08/2008):

- Initial Release

v1.1 (07/14/2008):

- Increased precision of position angles for RTN files from F6.1 to F12.7.

v1.2 (10/03/2008):

- BUG FIX: The drift between MAG and SC clocks resulted in falsely identified sample rate changes and assigned latencies.
- Modified format of MAGTable_Offsets.dat and associated read routine.
- Added file names of SCI, SHD, and LAC EDRs to release notes file.
- Added MAG offset determination from M2 MAG rolls.

v1.3 (10/02/2009):

- Updated msgr_kernel_getcurrent.pro to deal work with 3 and 4-digit version numbers.

- Fixed heater correction to include time lag between heater-on request and actual heater turn-on. Affected routines are: msgr_mag_edr2cdr_sci.pro, msgr_mag_correct_latency.pro, and msgr_mag_correct_heater100s.pro.

v1.4 (08/04/2010):

- Added processing of burst and AC channel data.
- Added handshake with SOC via semaphore file.

v1.5 (03/24/2011):

- Added handling of subversioned C-kernels.
- Added attitude rate change information to release notes.

v1.6 (04/15/2011):

- Added mechanism to automatically reprocess CDR files on arrival of updated C-kernels.

v1.7 (01/04/2012):

- Added temperature and heater duty cycle offset corrections as well as corrections for perturbations with 100 s heater period.

v1.8 (03/19/2012):

- Changed filename template for SPICE SPK kernel for compatibility with extended mission trajectory kernels.
- Added option for transformation to Venus Solar Orbital (VSO) coordinates.

v1.9 (10/17/2012):

- Updated numerous routines to accommodate for spacecraft clock roll-over (MET roll-over) on 8 January 2013.

v2.0 (04/15/2014):

- Added code to handle multiple versions of LAC data files.

v2.1 (05/22/2014):

- Added code to handle multiple versions of SCI data files. Added keyword to disable heater correction.

v3.0 (07/14/2015):

- First-iteration of complete thermal baseline correction.
- Hardcoded final SPICE kernels.

v3.1 – v3.6:

- Refinement of complete thermal baseline correction.

v3.7:

- Final complete thermal baseline correction.

15 References

Anderson, B. J. et al., The Magnetometer instrument on MESSENGER, *Space Sci. Rev.*, 131, 417-450, 2007.

16 Appendix

Tables 6-8 of the spline fits in units of counts or DN versus heater cycle time for the sensor axes, X, Y, and Z are given on the following pages.

Table 6: Average X-axis Heater Signal

t-sec	12%	16%	20%	24%	28%	32%	36%	40%
0	-0.70727	-0.60150	-0.38669	-0.21057	-0.20937	-0.01624	0.04162	0.21793
1	-0.76784	-0.93900	-0.32751	-0.28168	-0.22553	-0.13745	-0.18651	0.18604
2	-0.78477	-1.19015	-0.30390	-0.32659	-0.22482	-0.23701	-0.38173	0.14064
3	-0.77745	-1.34834	-0.31983	-0.34195	-0.22950	-0.31439	-0.55092	0.06758
4	-0.75217	-1.43091	-0.37269	-0.34284	-0.25425	-0.36909	-0.68744	-0.04287
5	-0.71527	-1.45920	-0.45793	-0.34614	-0.29884	-0.41328	-0.79610	-0.18103
6	-0.67305	-1.45453	-0.57103	-0.36876	-0.35570	-0.46532	-0.88729	-0.32769
7	-0.63257	-1.43827	-0.70747	-0.42754	-0.41723	-0.54363	-0.97147	-0.46356
8	-0.60665	-1.43350	-0.86754	-0.53515	-0.47916	-0.66565	-1.05934	-0.57287
9	-0.61087	-1.46639	-1.05993	-0.69695	-0.56307	-0.84141	-1.16359	-0.66682
10	-0.66078	-1.56339	-1.29418	-0.91754	-0.70254	-1.07749	-1.29783	-0.76913
11	-0.77198	-1.75097	-1.57983	-1.20153	-0.93120	-1.38044	-1.47568	-0.90359
12	-0.96002	-2.05521	-1.92621	-1.55330	-1.27429	-1.75197	-1.70682	-1.08920
13	-1.23556	-2.47475	-2.32680	-1.96220	-1.69651	-2.15886	-1.97270	-1.31043
14	-1.57423	-2.96295	-2.74894	-2.39274	-2.13598	-2.55253	-2.24232	-1.53656
15	-1.93652	-3.46894	-3.15751	-2.80712	-2.53070	-2.88436	-2.48464	-1.73681
16	-2.28287	-3.94183	-3.51740	-3.16754	-2.82623	-3.11276	-2.67197	-1.88436
17	-2.57371	-4.33111	-3.79381	-3.43654	-3.01933	-3.24408	-2.79914	-1.97908
18	-2.76947	-4.60730	-3.96940	-3.59772	-3.12799	-3.30448	-2.87030	-2.03191
19	-2.83671	-4.77339	-4.05378	-3.66720	-3.17026	-3.32022	-2.88968	-2.05383
20	-2.78159	-4.83516	-4.05887	-3.66384	-3.16284	-3.31478	-2.86334	-2.05508
21	-2.62599	-4.79839	-3.99662	-3.60653	-3.11382	-3.29406	-2.80925	-2.04119
22	-2.39185	-4.66881	-3.87893	-3.51405	-3.02786	-3.25709	-2.75003	-2.01584
23	-2.10111	-4.45040	-3.71801	-3.40057	-2.90967	-3.20287	-2.70830	-1.98271
24	-1.77569	-4.14459	-3.52640	-3.27360	-2.76514	-3.13059	-2.70213	-1.94552
25	-1.43607	-3.75261	-3.31666	-3.14014	-2.60741	-3.04045	-2.72228	-1.90812
26	-1.09410	-3.27570	-3.10139	-3.00717	-2.45232	-2.93307	-2.74943	-1.87444
27	-0.75851	-2.71543	-2.89284	-2.88152	-2.31570	-2.80904	-2.76421	-1.84842
28	-0.43802	-2.08868	-2.69018	-2.76291	-2.21000	-2.67008	-2.75016	-1.83306
29	-0.14134	-1.43296	-2.47490	-2.64148	-2.12863	-2.52418	-2.70699	-1.82615
30	0.12281	-0.78723	-2.22722	-2.50668	-2.05838	-2.38152	-2.64006	-1.82370
31	0.34707	-0.19046	-1.92736	-2.34797	-1.98601	-2.25227	-2.55474	-1.82168
32	0.53143	0.31892	-1.55618	-2.15492	-1.90037	-2.14426	-2.45564	-1.81593
33	0.67831	0.72265	-1.11767	-1.92134	-1.80134	-2.05278	-2.34340	-1.80142
34	0.79014	1.02796	-0.64510	-1.64646	-1.69244	-1.96903	-2.21733	-1.77283
35	0.86936	1.24371	-0.17363	-1.32982	-1.57719	-1.88419	-2.07676	-1.72487
36	0.91839	1.37879	0.26159	-0.97098	-1.45435	-1.78949	-1.92294	-1.65399
37	0.94016	1.44225	0.62610	-0.56980	-1.29908	-1.67623	-1.76676	-1.56540
38	0.94010	1.44934	0.90747	-0.13577	-1.07921	-1.53577	-1.62209	-1.46705
39	0.92435	1.42263	1.11938	0.31021	-0.76256	-1.35945	-1.50281	-1.36688
40	0.89910	1.38513	1.27703	0.74655	-0.33171	-1.14072	-1.41672	-1.27110
41	0.87049	1.35983	1.39560	1.15168	0.16166	-0.88282	-1.34329	-1.17793
42	0.84470	1.36916	1.49015	1.50442	0.64566	-0.59187	-1.25366	-1.08323
43	0.82668	1.41908	1.57145	1.79450	1.04840	-0.27398	-1.11900	-0.98287
44	0.81590	1.49734	1.64557	2.02371	1.31592	0.06281	-0.91841	-0.87286
45	0.81034	1.59073	1.71831	2.19449	1.47329	0.40200	-0.66613	-0.74989
46	0.80796	1.68604	1.79549	2.30930	1.56737	0.72473	-0.38606	-0.61083
47	0.80672	1.77013	1.88275	2.37074	1.64502	1.01218	-0.10211	-0.45257
48	0.80458	1.83134	1.98137	2.38561	1.74190	1.24974	0.16648	-0.27195
49	0.80022	1.85961	2.08812	2.36507	1.84709	1.44050	0.41975	-0.06581
50	0.79520	1.84492	2.19955	2.32049	1.93762	1.59210	0.66277	0.16903
51	0.79183	1.77728	2.31222	2.26322	1.99052	1.71221	0.90062	0.43575

52	0.79241	1.64767	2.42258	2.20427	1.99121	1.80767	1.13454	0.73251
53	0.79925	1.46913	2.52489	2.14633	1.95804	1.88218	1.35095	1.03779
54	0.81465	1.27617	2.61126	2.08407	1.91739	1.93864	1.53259	1.32526
55	0.83971	1.10417	2.67370	2.01180	1.89567	1.97996	1.66223	1.56859
56	0.87093	0.98854	2.70425	1.92386	1.90974	2.00904	1.73232	1.74832
57	0.90375	0.96280	2.69529	1.81505	1.94137	2.02866	1.77098	1.87032
58	0.93360	1.02410	2.64645	1.69003	1.96430	2.04158	1.81456	1.94629
59	0.95593	1.13635	2.56396	1.56238	1.95223	2.05056	1.89941	1.98791
60	0.96617	1.26222	2.45428	1.44606	1.88943	2.05744	2.04705	2.00577
61	0.96126	1.36442	2.32390	1.35499	1.79683	2.06075	2.22757	2.00662
62	0.94326	1.40760	2.17923	1.30235	1.70332	2.05837	2.39991	1.99637
63	0.91531	1.39103	2.02596	1.28815	1.63775	2.04812	2.52300	1.98092
64	0.88055	1.34361	1.86915	1.30115	1.61878	2.02936	2.56800	1.96486
65	0.84214	1.29515	1.71382	1.32973	1.63157	2.00636	2.54601	1.94842
66	0.80321	1.27550	1.56501	1.36227	1.65446	1.98439	2.47624	1.93094
67	0.76701	1.31251	1.42762	1.38770	1.66580	1.96871	2.37795	1.91175
68	0.73707	1.40265	1.30465	1.40336	1.64913	1.96150	2.26987	1.89004
69	0.71700	1.51726	1.19758	1.41333	1.60392	1.95545	2.16919	1.86447
70	0.71037	1.62698	1.10784	1.42191	1.53273	1.94143	2.09282	1.83362
71	0.72080	1.70243	1.03685	1.43337	1.43813	1.91031	2.05764	1.79605
72	0.75186	1.71621	0.98582	1.45146	1.32627	1.85752	2.07069	1.75068
73	0.80364	1.66923	0.95254	1.47202	1.21376	1.79178	2.11033	1.69747
74	0.86616	1.58359	0.93227	1.48501	1.11912	1.72422	2.14976	1.63654
75	0.92765	1.48193	0.92021	1.48024	1.06084	1.66595	2.16216	1.56803
76	0.97632	1.38688	0.91156	1.44750	1.04779	1.62391	2.13154	1.49361
77	1.00042	1.31948	0.90147	1.37753	1.06249	1.59355	2.07145	1.41923
78	0.98817	1.28019	0.88434	1.27293	1.08297	1.56836	2.00051	1.35155
79	0.93333	1.25498	0.85407	1.14468	1.08725	1.54188	1.93729	1.29720
80	0.84412	1.22954	0.80455	1.00393	1.06016	1.50938	1.89344	1.25773
81	0.73109	1.18954	0.72966	0.86182	1.00400	1.47085	1.86259	1.22137
82	0.60481	1.12219	0.62452	0.72911	0.92390	1.42698	1.83553	1.17428
83	0.47585	1.03284	0.49885	0.61194	0.82496	1.37848	1.80303	1.10261
84	0.35477	0.93872	0.37194	0.51338	0.71392	1.32671	1.75815	0.99993
85	0.24874	0.85729	0.26327	0.43648	0.60137	1.27466	1.69948	0.87789
86	0.15686	0.80601	0.19232	0.38427	0.49851	1.22552	1.62646	0.75087
87	0.07700	0.80038	0.17598	0.35908	0.41650	1.18252	1.53852	0.63323
88	0.00705	0.83477	0.20328	0.35563	0.36122	1.14618	1.43843	0.53542
89	-0.05511	0.89054	0.24612	0.36393	0.32625	1.11087	1.33658	0.45886
90	-0.11161	0.94886	0.27615	0.37394	0.30345	1.07009	1.24447	0.40370
91	-0.16447	0.99092	0.26501	0.37561	0.28469	1.01736	1.17354	0.37007
92	-0.21560	0.99878	0.18781	0.35966	0.26262	0.94831	1.12584	0.35533
93	-0.26686	0.96334	0.05418	0.32432	0.23158	0.86320	1.08295	0.35080
94	-0.32011	0.88059	-0.10642	0.27214	0.18613	0.76289	1.02372	0.34700
95	-0.37721	0.74656	-0.26430	0.20572	0.12089	0.64826	0.92710	0.33447
96	-0.44003	0.55731	-0.38977	0.12768	0.03679	0.52139	0.78366	0.30906
97	-0.50819	0.31072	-0.45638	0.04089	-0.05225	0.38679	0.60805	0.27756
98	-0.57687	0.02152	-0.46721	-0.04926	-0.13065	0.24932	0.41788	0.24810
99	-0.64065	-0.28651	-0.44123	-0.13606	-0.18293	0.11379	0.23072	0.22876
100	-0.70727	-0.60150	-0.38669	-0.21057	-0.20937	-0.01624	0.04162	0.21793

Table 7: Average Y-axis Heater Signal

t-sec	12%	16%	20%	24%	28%	32%	36%	40%
0	-0.67866	-0.80900	-0.35343	-0.81213	-0.47221	-0.41136	-0.33629	-0.04096
1	-1.15441	-1.34476	-0.78112	-0.92012	-0.74668	-0.66317	-0.57261	-0.23571
2	-1.53719	-1.74938	-1.22589	-1.02648	-1.00495	-0.89633	-0.79972	-0.43465
3	-1.81474	-1.99454	-1.60228	-1.14063	-1.23201	-1.11973	-1.03795	-0.63785
4	-2.00501	-2.11974	-1.83997	-1.26890	-1.40897	-1.33113	-1.28674	-0.84793
5	-2.13117	-2.17244	-1.94799	-1.40572	-1.54537	-1.52966	-1.53635	-1.06461
6	-2.21635	-2.20015	-1.97438	-1.53966	-1.66470	-1.71511	-1.77250	-1.28626
7	-2.28391	-2.25034	-1.96741	-1.65926	-1.79051	-1.88728	-1.98089	-1.51119
8	-2.37299	-2.36947	-1.97948	-1.76254	-1.94998	-2.05254	-2.15413	-1.74058
9	-2.55067	-2.60225	-2.09459	-1.92047	-2.19797	-2.26781	-2.33794	-1.99744
10	-2.88689	-2.99321	-2.41143	-2.23788	-2.60217	-2.61346	-2.60273	-2.31491
11	-3.45159	-3.58687	-3.02876	-2.81981	-3.23036	-3.17001	-3.01900	-2.72617
12	-4.31359	-4.42690	-4.01805	-3.74526	-4.12984	-3.99613	-3.64050	-3.25469
13	-5.46257	-5.49712	-5.25398	-4.90560	-5.20023	-4.99288	-4.39973	-3.85363
14	-6.75762	-6.68254	-6.52482	-6.10984	-6.27633	-5.99217	-5.17605	-4.44531
15	-8.04564	-7.85894	-7.61849	-7.16663	-7.19268	-6.82559	-5.84856	-4.95191
16	-9.17348	-8.90210	-8.35215	-7.90972	-7.80639	-7.34895	-6.31214	-5.30685
17	-9.98918	-9.68895	-8.74095	-8.34282	-8.12755	-7.58204	-6.56849	-5.51950
18	-10.40830	-10.16450	-8.88215	-8.54011	-8.22968	-7.61263	-6.66363	-5.63075
19	-10.45080	-10.37870	-8.87326	-8.57600	-8.18652	-7.52870	-6.64371	-5.68161
20	-10.14550	-10.39050	-8.80165	-8.51883	-8.06501	-7.40860	-6.55186	-5.70782
21	-9.52117	-10.25910	-8.68997	-8.39840	-7.88884	-7.26912	-6.41194	-5.71177
22	-8.60708	-10.04250	-8.53554	-8.22939	-7.66478	-7.10298	-6.24029	-5.68279
23	-7.45616	-9.75401	-8.33560	-8.02645	-7.39953	-6.90283	-6.05321	-5.61018
24	-6.15539	-9.34247	-8.08786	-7.80390	-7.10032	-6.66366	-5.86450	-5.48652
25	-4.79444	-8.75161	-7.79277	-7.57410	-6.77733	-6.39431	-5.67299	-5.32414
26	-3.46297	-7.92516	-7.45178	-7.34866	-6.44185	-6.10876	-5.47196	-5.14266
27	-2.24968	-6.80866	-7.06634	-7.13921	-6.10515	-5.82102	-5.25468	-4.96172
28	-1.20381	-5.42369	-6.63051	-6.95096	-5.77640	-5.54219	-5.01621	-4.79703
29	-0.32116	-3.89463	-6.09682	-6.75310	-5.45274	-5.26718	-4.76177	-4.64223
30	0.40626	-2.35314	-5.40329	-6.50225	-5.12717	-4.98526	-4.50009	-4.48327
31	0.98640	-0.93089	-4.48792	-6.15500	-4.79266	-4.68568	-4.23991	-4.30608
32	1.42742	0.24266	-3.31444	-5.67102	-4.44335	-4.36106	-3.98803	-4.09952
33	1.74380	1.11842	-1.98255	-5.02615	-4.07954	-4.02178	-3.74093	-3.86793
34	1.95800	1.74903	-0.63672	-4.20158	-3.70358	-3.68404	-3.49168	-3.62074
35	2.09301	2.19366	0.57855	-3.17846	-3.31781	-3.36406	-3.23337	-3.36737
36	2.17182	2.51147	1.54382	-1.95811	-2.91636	-3.07130	-2.96054	-3.11577
37	2.21727	2.76080	2.26425	-0.64195	-2.45254	-2.78150	-2.67498	-2.86648
38	2.24736	2.97364	2.78371	0.63750	-1.86699	-2.45995	-2.38076	-2.61772
39	2.27440	3.15075	3.14605	1.74772	-1.10034	-2.07194	-2.08194	-2.36774
40	2.31034	3.29107	3.39378	2.58523	-0.12101	-1.58848	-1.78075	-2.11522
41	2.36715	3.39355	3.56296	3.18256	0.97254	-1.00737	-1.47089	-1.86094
42	2.45633	3.45732	3.68779	3.61202	2.04380	-0.33427	-1.14356	-1.60627
43	2.57683	3.48681	3.80246	3.94593	2.95623	0.42519	-0.78995	-1.35259
44	2.71358	3.49231	3.93224	4.24403	3.60526	1.25599	-0.40109	-1.09839
45	2.85082	3.48441	4.06303	4.51057	4.02711	2.10179	0.03281	-0.82940
46	2.97276	3.47372	4.16990	4.73450	4.29684	2.89485	0.52173	-0.52782
47	3.06407	3.47059	4.22791	4.90478	4.48949	3.56745	1.07566	-0.17585
48	3.12016	3.47955	4.21994	5.01521	4.66579	4.06880	1.69424	0.23991
49	3.14766	3.49904	4.16137	5.07971	4.82703	4.41846	2.33402	0.71456
50	3.15370	3.52722	4.07604	5.11740	4.95905	4.65426	2.94040	1.23845

51	3.14541	3.56225	3.98775	5.14741	5.04772	4.81402	3.45877	1.80196
52	3.12981	3.60218	3.91624	5.18171	5.08366	4.92950	3.84950	2.39045
53	3.11091	3.64242	3.86525	5.20424	5.07620	5.00878	4.13161	2.96980
54	3.08984	3.67584	3.83464	5.19207	5.03923	5.05410	4.33842	3.50112
55	3.06761	3.69521	3.82424	5.12230	4.98665	5.06776	4.50325	3.94551
56	3.04523	3.69327	3.83204	4.98243	4.92949	5.05280	4.65170	4.27505
57	3.02350	3.66330	3.84917	4.79839	4.86833	5.01522	4.78083	4.50217
58	2.99962	3.60837	3.86523	4.60494	4.80135	4.96168	4.88114	4.64860
59	2.96742	3.54052	3.86978	4.43685	4.72669	4.89885	4.94313	4.73606
60	2.92063	3.47213	3.85726	4.32001	4.64336	4.83188	4.96124	4.78444
61	2.85297	3.41556	3.83900	4.24959	4.55325	4.76067	4.94353	4.80713
62	2.75876	3.38253	3.83001	4.21407	4.45888	4.68401	4.90104	4.81617
63	2.64272	3.37314	3.84527	4.20193	4.36276	4.60065	4.84482	4.82356
64	2.51848	3.37755	3.88921	4.19989	4.26605	4.50992	4.78345	4.83519
65	2.39993	3.38560	3.93179	4.18889	4.16539	4.41292	4.71757	4.83697
66	2.30099	3.38715	3.93589	4.14866	4.05653	4.31113	4.64621	4.81068
67	2.23472	3.37238	3.86442	4.05895	3.93521	4.20603	4.56837	4.73816
68	2.20089	3.33688	3.70017	3.91072	3.80001	4.09915	4.48318	4.60948
69	2.18858	3.28054	3.48719	3.72938	3.65825	3.99231	4.39009	4.44022
70	2.18658	3.20341	3.28129	3.54699	3.51893	3.88735	4.28858	4.25087
71	2.18367	3.10551	3.13826	3.39558	3.39103	3.78612	4.17817	4.06190
72	2.16904	2.98716	3.08792	3.29500	3.28048	3.68921	4.05970	3.88897
73	2.13743	2.85287	3.08463	3.22958	3.18424	3.59360	3.93782	3.73370
74	2.08775	2.71029	3.06911	3.17726	3.09770	3.49561	3.81790	3.59520
75	2.01901	2.56712	2.98211	3.11599	3.01621	3.39156	3.70531	3.47255
76	1.93022	2.43111	2.79204	3.02976	2.93545	3.27837	3.60201	3.36429
77	1.82126	2.30960	2.54314	2.91913	2.85199	3.15462	3.50072	3.26740
78	1.70302	2.20522	2.29257	2.78749	2.76252	3.01914	3.39255	3.17857
79	1.59417	2.11725	2.09741	2.63824	2.66376	2.87081	3.26863	3.09451
80	1.51353	2.04491	1.98790	2.47617	2.55271	2.71156	3.12231	3.01038
81	1.47994	1.98743	1.92481	2.30975	2.42715	2.55140	2.95263	2.91724
82	1.50970	1.94378	1.85781	2.14801	2.28499	2.40159	2.75959	2.80556
83	1.58929	1.91011	1.73666	1.99998	2.12416	2.27340	2.54317	2.66579
84	1.68558	1.88071	1.53674	1.86961	1.94694	2.17094	2.30801	2.49511
85	1.76509	1.84981	1.29616	1.74851	1.76628	2.08092	2.07015	2.30713
86	1.79435	1.81168	1.06240	1.62642	1.59672	1.98740	1.84734	2.11792
87	1.74342	1.76122	0.88290	1.49309	1.45280	1.87449	1.65728	1.94352
88	1.62072	1.70070	0.78306	1.34102	1.34063	1.73382	1.50788	1.79325
89	1.45827	1.63687	0.73741	1.16910	1.24695	1.57437	1.38441	1.66086
90	1.28840	1.57653	0.71333	0.97709	1.15577	1.40756	1.26894	1.53788
91	1.14348	1.52650	0.67827	0.76478	1.05113	1.24479	1.14358	1.41590
92	1.05175	1.49135	0.61438	0.53504	0.92408	1.09209	0.99807	1.28808
93	1.00064	1.45310	0.53597	0.29748	0.78101	0.94378	0.83877	1.15111
94	0.95414	1.38088	0.46161	0.06259	0.63034	0.79260	0.67428	1.00216
95	0.87595	1.24365	0.40971	-0.15913	0.48043	0.63133	0.51312	0.83839
96	0.72978	1.01035	0.37933	-0.35841	0.33317	0.45499	0.35908	0.66034
97	0.48388	0.65529	0.32954	-0.52847	0.17700	0.26322	0.20609	0.47541
98	0.14827	0.20154	0.21444	-0.66284	-0.00128	0.05625	0.04687	0.29186
99	-0.24463	-0.30163	-0.01158	-0.75515	-0.21479	-0.16568	-0.12583	0.11791
100	-0.67866	-0.80900	-0.35343	-0.81213	-0.47221	-0.41136	-0.33629	-0.04096

Table 8: Average Z-axis Heater Signal

t-sec	12%	16%	20%	24%	28%	32%	36%	40%
0	0.03662	0.00357	-0.30056	0.01204	-0.06795	0.24396	0.09263	0.53584
1	-0.01090	-0.07881	-0.32656	0.05595	-0.12833	0.25216	0.08109	0.33415
2	0.02221	-0.19520	-0.29570	0.07581	-0.17689	0.24295	0.07408	0.14172
3	0.08079	-0.28267	-0.23967	0.05514	-0.19805	0.22733	0.06344	-0.02584
4	0.15040	-0.34358	-0.17285	0.00325	-0.18257	0.20389	0.03967	-0.14756
5	0.21660	-0.38170	-0.11052	-0.06825	-0.13356	0.17573	0.00164	-0.22578
6	0.26498	-0.40077	-0.06797	-0.14771	-0.06017	0.14815	-0.04769	-0.27424
7	0.28279	-0.40458	-0.06038	-0.22360	0.02840	0.12644	-0.10533	-0.30676
8	0.27055	-0.40025	-0.09635	-0.29240	0.12105	0.11431	-0.16863	-0.33619
9	0.23502	-0.40077	-0.17275	-0.36477	0.19183	0.10299	-0.23772	-0.36769
10	0.18297	-0.41975	-0.28529	-0.45279	0.20795	0.07796	-0.31397	-0.40287
11	0.12121	-0.47081	-0.42965	-0.56857	0.13657	0.02466	-0.39878	-0.44332
12	0.05651	-0.56734	-0.60144	-0.72402	-0.04763	-0.06877	-0.49265	-0.49046
13	-0.00520	-0.70950	-0.79048	-0.91813	-0.31566	-0.19460	-0.58967	-0.54427
14	-0.06416	-0.87554	-0.97700	-1.12856	-0.61466	-0.33655	-0.68110	-0.60414
15	-0.12326	-1.04165	-1.14034	-1.33098	-0.89170	-0.47825	-0.75822	-0.66942
16	-0.18540	-1.18404	-1.25986	-1.50106	-1.10025	-0.60483	-0.81371	-0.73974
17	-0.25350	-1.27912	-1.31518	-1.61473	-1.23703	-0.71117	-0.84997	-0.81635
18	-0.33047	-1.31688	-1.30349	-1.66323	-1.31675	-0.79620	-0.87339	-0.90117
19	-0.41745	-1.30819	-1.24904	-1.66141	-1.35416	-0.85889	-0.89042	-0.99611
20	-0.50432	-1.26575	-1.17839	-1.62614	-1.36290	-0.89870	-0.90664	-1.10149
21	-0.57645	-1.20221	-1.11810	-1.57431	-1.34952	-0.91834	-0.92238	-1.20733
22	-0.61921	-1.13010	-1.09440	-1.52263	-1.31778	-0.92179	-0.93591	-1.29960
23	-0.61795	-1.05402	-1.11668	-1.47933	-1.27144	-0.91303	-0.94550	-1.36429
24	-0.55804	-0.96716	-1.16998	-1.44044	-1.21470	-0.89635	-0.94979	-1.38957
25	-0.42907	-0.86182	-1.23747	-1.40100	-1.15435	-0.87788	-0.94955	-1.37675
26	-0.24543	-0.73030	-1.30231	-1.35611	-1.09815	-0.86444	-0.94639	-1.33201
27	-0.03057	-0.56515	-1.34779	-1.30092	-1.05385	-0.86284	-0.94190	-1.26154
28	0.19204	-0.36989	-1.36199	-1.23563	-1.02693	-0.87767	-0.93698	-1.17222
29	0.39894	-0.16284	-1.33956	-1.16716	-1.01014	-0.90091	-0.92861	-1.07492
30	0.56667	0.03662	-1.27558	-1.10294	-0.99176	-0.92018	-0.91240	-0.98190
31	0.67659	0.20912	-1.16515	-1.05038	-0.96005	-0.92308	-0.88396	-0.90541
32	0.73604	0.33562	-1.00370	-1.01663	-0.90673	-0.90027	-0.84060	-0.85523
33	0.76101	0.40932	-0.79950	-0.99973	-0.84164	-0.85855	-0.78848	-0.82794
34	0.76749	0.43890	-0.57703	-0.98614	-0.78059	-0.81008	-0.73674	-0.81581
35	0.77149	0.43405	-0.36181	-0.96155	-0.73938	-0.76699	-0.69449	-0.81108
36	0.78901	0.40445	-0.17937	-0.91169	-0.72868	-0.73871	-0.66914	-0.80666
37	0.83174	0.35976	-0.05450	-0.82270	-0.73341	-0.72124	-0.65963	-0.79870
38	0.89029	0.30884	0.01121	-0.69420	-0.73054	-0.70640	-0.66225	-0.78437
39	0.94880	0.25964	0.04365	-0.54181	-0.69703	-0.68600	-0.67329	-0.76080
40	0.99143	0.22001	0.07033	-0.38210	-0.61549	-0.65231	-0.68819	-0.72589
41	1.00232	0.19786	0.11875	-0.23161	-0.49503	-0.59975	-0.69836	-0.68096
42	0.96563	0.20076	0.21548	-0.10645	-0.35252	-0.52331	-0.69402	-0.62836
43	0.87019	0.22795	0.36175	-0.01015	-0.20480	-0.41803	-0.66538	-0.57040
44	0.72592	0.26945	0.53060	0.06769	-0.06673	-0.28260	-0.60544	-0.50919
45	0.54858	0.31477	0.69363	0.13818	0.05575	-0.13192	-0.51929	-0.44572
46	0.35397	0.35344	0.82240	0.21246	0.15913	0.01465	-0.41539	-0.38073
47	0.15786	0.37534	0.88945	0.30126	0.23990	0.13773	-0.30220	-0.31493
48	-0.02395	0.37956	0.89054	0.40537	0.29681	0.22314	-0.18690	-0.24842
49	-0.17833	0.37471	0.84560	0.51529	0.33790	0.27821	-0.07141	-0.17871
50	-0.30291	0.36988	0.77569	0.62102	0.37365	0.31585	0.04370	-0.10264

51	-0.39810	0.37412	0.70189	0.71256	0.41452	0.34898	0.15788	-0.01706
52	-0.46428	0.39605	0.64467	0.78026	0.46760	0.38741	0.27013	0.07978
53	-0.50186	0.43435	0.61213	0.82187	0.52673	0.42884	0.37775	0.18408
54	-0.51123	0.47796	0.60023	0.84232	0.58249	0.46802	0.47760	0.29067
55	-0.49445	0.51547	0.60443	0.84687	0.62550	0.49969	0.56657	0.39439
56	-0.45978	0.53543	0.62023	0.84077	0.64895	0.51984	0.64278	0.49057
57	-0.41692	0.52696	0.64299	0.82924	0.65561	0.52905	0.70893	0.57634
58	-0.37558	0.49013	0.66644	0.81724	0.65048	0.52896	0.76883	0.64925
59	-0.34548	0.43499	0.68276	0.80945	0.63853	0.52120	0.82623	0.70685
60	-0.33630	0.37196	0.68410	0.81055	0.62385	0.50810	0.88382	0.74654
61	-0.35402	0.31146	0.66258	0.82523	0.60746	0.49431	0.94046	0.76531
62	-0.39178	0.26348	0.61103	0.85778	0.58968	0.48498	0.99419	0.76003
63	-0.44000	0.23045	0.53442	0.90580	0.57085	0.48528	1.04305	0.72757
64	-0.48911	0.20833	0.44807	0.96119	0.55273	0.49759	1.08435	0.66952
65	-0.52951	0.19288	0.36764	1.01563	0.54174	0.51526	1.11303	0.60290
66	-0.55163	0.17986	0.30882	1.06083	0.54526	0.52975	1.12354	0.54784
67	-0.54870	0.16527	0.28652	1.08887	0.57066	0.53258	1.11036	0.52450
68	-0.52283	0.14899	0.30372	1.09810	0.62050	0.51866	1.07123	0.54423
69	-0.47780	0.13404	0.35388	1.09187	0.68252	0.49357	1.01410	0.59122
70	-0.41745	0.12351	0.43019	1.07364	0.74162	0.46490	0.94885	0.64448
71	-0.34556	0.12048	0.52581	1.04693	0.78268	0.44025	0.88537	0.68300
72	-0.26597	0.12773	0.63350	1.01515	0.79669	0.42460	0.83058	0.69397
73	-0.18311	0.14354	0.73976	0.98119	0.79231	0.41528	0.78269	0.68830
74	-0.10326	0.16279	0.82640	0.94746	0.78140	0.40822	0.73838	0.68121
75	-0.03303	0.18027	0.87512	0.91638	0.77579	0.39939	0.69432	0.68789
76	0.02096	0.19080	0.86762	0.89037	0.78207	0.38687	0.64847	0.71625
77	0.05213	0.18966	0.78780	0.87147	0.79233	0.37460	0.60236	0.75421
78	0.05386	0.17843	0.64804	0.85697	0.79621	0.36751	0.55814	0.78627
79	0.02384	0.16314	0.48076	0.84085	0.78338	0.37055	0.51795	0.79696
80	-0.02904	0.14991	0.31879	0.81697	0.74879	0.38510	0.48309	0.77725
81	-0.09406	0.14484	0.19496	0.77924	0.70111	0.40342	0.45278	0.73481
82	-0.16050	0.15350	0.13962	0.72241	0.65124	0.41631	0.42589	0.67995
83	-0.21765	0.17508	0.15386	0.65165	0.61002	0.41458	0.40127	0.62302
84	-0.25479	0.20454	0.21949	0.57895	0.58383	0.39488	0.37779	0.57396
85	-0.26525	0.23678	0.31801	0.51644	0.56813	0.36809	0.35432	0.54176
86	-0.25208	0.26671	0.43091	0.47623	0.55671	0.34727	0.32974	0.53530
87	-0.21973	0.28974	0.54006	0.46874	0.54336	0.34540	0.30292	0.56342
88	-0.17270	0.30686	0.63147	0.48590	0.52372	0.36767	0.27471	0.62807
89	-0.11544	0.32252	0.69370	0.50831	0.49762	0.40110	0.25050	0.71525
90	-0.05244	0.34120	0.71532	0.51639	0.46550	0.43016	0.23633	0.80875
91	0.01185	0.36738	0.68494	0.49054	0.42780	0.43938	0.23821	0.89236
92	0.07300	0.40447	0.59319	0.41386	0.38513	0.42090	0.25684	0.95462
93	0.12659	0.44488	0.45118	0.29591	0.33850	0.38356	0.28140	0.99445
94	0.16820	0.47477	0.28176	0.16148	0.28898	0.33840	0.29952	1.01210
95	0.19340	0.48020	0.10791	0.03554	0.23763	0.29642	0.29887	1.00786
96	0.19781	0.44725	-0.04736	-0.05695	0.18466	0.26500	0.27360	0.98031
97	0.18084	0.36424	-0.16299	-0.09398	0.12852	0.24396	0.23122	0.92459
98	0.14969	0.24027	-0.23551	-0.08079	0.06745	0.23220	0.18088	0.83543
99	0.11251	0.09557	-0.27091	-0.03722	-0.00031	0.22861	0.13174	0.70759
100	0.03662	0.00357	-0.30056	0.01204	-0.06795	0.24396	0.09263	0.53584